Systematic Control of Particle Size in Rapid Open-Vessel Microwave Synthesis of K-OMS-2 Nanofibers

Edward K. Nyutu,[‡] Chun-Hu Chen,[‡] Shanthakumar Sithambaram,[‡] Vincent Mark B. Crisostomo,[‡] and Steven L. Suib*[,‡,†]

Department of Chemistry and Department of Chemical, Materials and Bimolecular Engineering, University of Connecticut, Storrs, Connecticut 06269

Received: January 23, 2008; In Final Form: February 29, 2008

Multigram quantities of manganese oxide (K-OMS-2) nanomaterials in the size range of 4−20 nm and with very high surface areas up to 227 m^2/g were produced rapidly via microwave-reflux route with use of mixed aqueous and nonaqueous solvents. The formation process, particle size, crystallite size, crystal structure, and properties of these nanomaterials were characterized by X-ray diffraction, scanning electron microscopy (SEM), transmission electron microscopy (TEM), thermogravimetric analysis (TGA), differential scanning calorimetry (DSC), infrared spectroscopy (FT-IR), Raman spectroscopy, and nitrogen adsorption−desorption. The OMS-2 nanofiber diameter was systematically controlled by varying the concentration or type of the cosolvent. Catalytic studies of these K-OMS-2 nanomaterials for oxidation of anisyl alcohol were performed. These nanomaterials show excellent catalytic activity when compared with conventionally prepared bulk OMS-2 catalysts.

Introduction

Tremendous efforts have been made toward controlling the particle size, shape, and structure of inorganic nanomaterials.[1] One-dimensional (1D) transition metal oxide nanostructures (rods, wires, tubes, ribbons, fibers) are of special interest due to their unique catalytic, electronic, optical, thermal, and photonic properties intrinsically associated with their low dimensionality and the quantum confinement effect.[1−3] Cryptomelane-type manganese oxide (OMS-2) is a group of OMS family with a 2 × 2 tunnel structure with a pore size of 4.6 Å.[2,4−6] Their structures are constructed from edge-shared double chains of [MnO_6] octahedra, which are corner-connected to form one-dimensional (1D) tunnel structures as illustrated in Figure 1. These materials are a subject of intense research as low cost, efficient, and environmentally friendly materials with applications in gas sensing, catalysis, energy storage, separation (molecular sieves), and battery materials.[2,5]

The syntheses of K-OMS-2 nanomaterials takes several hours to several days, sometimes requiring multiple procedures under hydrothermal, conventional refluxing, and solid-state conditions with limited control over particle properties.[2,5−6] Recently, Villegas et al. prepared nanosize K-OMS-2 fibers with small particle sizes (6 nm) by reduction of $KMnO_4$ with H_2O_2 in acidic condition followed by heating under standard oil-bath refluxing for at least 15 h.[2] Even though particle size control was achieved by varying the amount of hydrogen peroxide, the surface area of these nanomaterial was less than 80 m^2/g and transformation from poorly ordered OMS to orderly tunnel type K-OMS-2 required longer refluxing times in excess of 15 h. Ding et al. recently synthesized OMS-2 nanorods (10 nm) by a solvent-free method.[5h] The solvent-free route produced high surface area (∼156 m^2/g) OMS-2 nanomaterials in hours (>1 h). However, particle size control was not accomplished with this method.

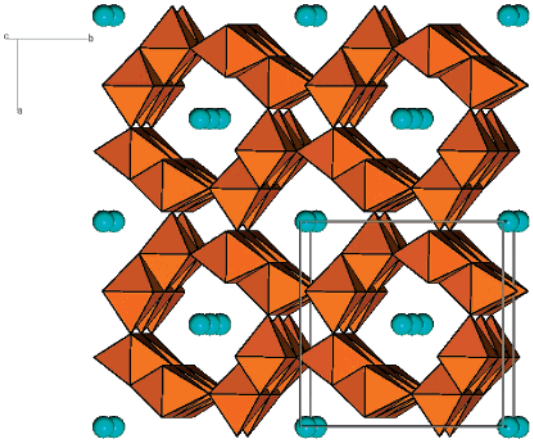

Figure 1. Crystal structure of cryptomelane-type OMS-2: potassium atoms are shown as blue spheres; MnO_6 octahedra are shown in brown.

Microwave heating has been employed in many chemical reactions and has been found to be more effective in selective heating in many processes.[7] Microwave-enhanced chemistry is based on the interactions of dielectric materials, liquids, or solid with microwave radiation that causes dielectric heating. The electric dipoles present in these materials respond to the applied electromagnetic field. In liquids, the heating rate of solvents under microwave irradiation depends on their dielectric constant (ϵ'') and dielectric loss (ϵ') that is given by (ϵ''/ϵ'), defined as the energy dissipation factor or loss tangent (tan δ).[7a−c] Water has a medium dielectric loss (tan $\delta = 0.123$) and is an excellent solvent for microwave-assisted synthesis. Dimethy sulfoxide (DMSO) has a higher tan $\delta = 0.825$ and will absorb microwave irradiation more efficiently than water resulting in superheating.[7b,c] Synthesis of OMS-2 materials has been investigated extensively by using traditional oil-bath refluxing, often requiring long crystallization periods (>17 h).[2,5−6] Dramatic crystallization rate enhancements are expected when high microwave absorbing solvents are heated by microwave irradiation at atmospheric

* To whom correspondence should be addressed. Phone: 860-486-2797. Fax: 860-486-2981. E-mail: steve.suib@uconn.edu.
‡ Department of Chemistry.
† Department of Chemical, Materials and Bimolecular Engineering.

10.1021/jp800672m CCC: $40.75
Published on Web 04/10/2008

pressure in an open vessel (microwave-refluxing). Without the superheating or other nonthermal effects at atmospheric pressure, the expected rate enhancements would be relatively small.[7b]

In this article, studies on rapid multigram production and particle size control of OMS-2 nanomaterials are investigated. Since different solute−solvent interactions are expected under microwave irradiation with different solvent systems, rapid production and systematic particle control study of K-OMS-2 nanomaterials were studied.

Experimental Section

Materials. Potassium permanganate ($KMnO_4$) and manganese sulfate monohydrate ($MnSO_4 \cdot H_2O$) were obtained from Sigma-Aldrich. Nitric acid 70% (HNO_3) was obtained from Alfa Aesar. The solvents dimethyl sulfoxide (DMSO) (99.9%, Acros), *N*,*N*-dimethylformamide (DMF) (ACS reagent, J. T. Baker), ethylene glycol (EG), propylene glycol (PG), sulfolane, dimethylacetamide (DMA) (ACS reagent, Fluka), ethanol, *N*-methyl pyrrolidone (NMP), and ethyl acetate used in this research were obtained from commercial sources and used without further purification.

Synthesis. K-OMS-2 nanomaterials were prepared by the microwave-reflux method, using comproportionation[8] between Mn^{2+} and Mn^{7+} precursors in mixed aqueous and nonaqueous solvents under acidic media. This method involves a variation of the procedure reported by DeGuzman et al. for the preparation of synthetic cryptomelane.[5c] In a typical reaction, 42 mmol (6.65 g) of $KMnO_4$ in 100 mL of distilled−deionized water (DDW) was added dropwise to a mixture of 59 mmol (9.9 g) of $MnSO_4 \cdot H_2O$ dissolved in 33 mL of DDW and 3.4 mL of concentrated HNO_3 under constant stirring for 15 min. To make a 10% (v/v) DMSO solution, 15 mL of dimethylsulfoxide was added to the mixture. The resulting brownish mixture was transferred into a 250 cm^3 round-bottomed flask and placed in a multimode CEM MARS 5 Microwave Chamber fitted with a reflux condenser, stirring capability employing a Teflon coated magnetic stirrer, and a fiber-optic probe temperature-measuring device directly inserted into the reaction mixture by means of a sapphire thermowell (Figure S1 in the Supporting Information).

The microwave power was set to 100% of 300 W but fluctuated in order to maintain the input temperature value of 100 ± 2 °C, ramp rate 20 deg/min, and 0−120 min hold time. The resulting black product was filtered, washed thoroughly with DDW, dried under vacuum overnight, and oven dried to further remove water at 80 °C for 1 h. The OMS-2 prepared by this method with 10% DMSO as a cosolvent for 90 min is referred to as MR (microwave-reflux)-90−10% DMSO and MR-90−0% DMSO; conventional OMS-2 recipe but under microwave-refluxing for 90 min instead of oil-bath refluxing. The concentration of DMSO in the reaction was varied between 0 and 50% (v/v). Typical yields were ∼70% for 10% DMSO cosolvent (MR-90−10% DMSO) and >90% when 10% sulfolane was used as a cosolvent (MR-90−10% sulfolane).

To investigate the nature of the cosolvent in the reaction media in the crystallization process and particle size control, K-OMS-2 materials were synthesized from $KMnO_4$ and $MnSO_4 \cdot H_2O$ as previously described but using different cosolvents at a concentration of 10% (v/v). The cosolvents investigated in this study include the following: ethanol, ethylene glycol, propylene glycol, sulfolane, DMF, NMP, and ethyl acetate. Though solvents used in this study are relatively safe, caution should be taken when handling these solvents particularly for large-scale production of OMS-2 nanomaterials. Closed vessels containing volatile solvents and permanganates can produce an explosion. Microwaves create hot spots that can accelerate the explosion. Readers are advised to take appropriate safety and handling precautions.

Characterization Methods. The powder X-ray diffraction studies were performed with a Scintag XDS-2000 diffractometer using Cu Kα ($\lambda = 0.15406$ nm) radiation. A beam voltage of 45 kV and a 40 mA beam current were used. The data were collected in the 2θ range 5−70° with a continuous scan rate of 0.5 deg/min and the phases identified by using the Joint Committee on powder diffraction society (JCPDS) database. The XRD patterns of samples were collected on aluminum holder. The crystalline particle size of the prepared OMS materials was determined using the Debye−Scherer equation[9] with the integral widths corrected with LaB_6 standard. For this analysis, the (310), (211), and (411) reflections of the Q-phase cryptomelane-type MnO_2 were utilized.[2] The morphology of the products was studied by field emission scanning electron microscopy (FE-SEM) on a Zeiss DSM 982 Gemini instrument with a Schottky emitter at an accelerating voltage of 2 kV and a beam current of 1 mA. The samples were suspended in water and dispersed on Au−Pd-coated silicon chips previously mounted onto stainless-steel sample holders with two-sided carbon tape. TEM and HRTEM studies were carried out with a JEOL 2010 UHR FasTEM operating at an accelerating voltage of 200 kV and equipped with an energy dispersive X-ray analysis (EDXS) system. The samples were prepared by dispersing the material in 2-propanol. A drop of the dispersion was placed onto a carbon-coated copper grid and allowed to dry. The properties of the prepared materials were studied by FT-IR, using a Nicolet Magna-IR Model 750 in the range 4000−400 cm^{-1} with a DTGS detector. The dark manganese oxide powders were diluted with KBr at a ratio of 1:100 and then pressed into pellets at about 10 000 psi. The spectral background was collected with pure KBr discs. Raman measurements of the OMS-2 prepared with and without the cosolvent were taken at room temperature on a Renishaw 2000 Ramascope attached to a CCD camera with a 514.5 nm Ar^+ laser as the excitation source. Prior to each measurement the spectrometer was calibrated with a silicon wafer. Thermogravimetric analysis (TGA) and differential scanning calorimetry (DSC) were employed to study the thermal stability of the samples. The TGA experiments were performed with a Hi-Res TA instrument Model 2950. Differential scanning calorimetry (DSC) experiments were done on a DSC Model Q100. The temperature ramp for TGA and DSC was 20 deg/min in nitrogen atmosphere. The nitrogen sorption experiments were performed with a Micrometrics ASAP 2010 accelerated surface area system. The adsorption and desorption experiments were carried out at 77 K with samples previously degassed at 120 °C for 12 h. The specific surface area of the samples was determined by the Brunauer−Emmett−Teller (BET) method. The micropore and mesopore size distributions were calculated by Horvath−Kawazoe (HK) and Barrett−Joyner−Halenda (BJH) methods, respectively.[10]

Catalytic Applications. The anisyl alcohol (4-methoxybenzyl alcohol, 98%) was purchased from Sigma-Aldrich and used without further purification. The heterogeneous liquid oxidation reactions were performed in a batch reactor. To a 50 mL, two-necked round-bottomed flask, 50 mg of manganese oxide catalyst was added along with 1 mmol of 4-methoxy benzyl alcohol and 10 mL of toluene as solvent. The reaction mixture was stirred and refluxed in an oil-bath at 100 °C under an air atmosphere for 4 h.

The quantitative analysis and identification of the reaction products was performed by GC-MS, using a HP 5971 mass

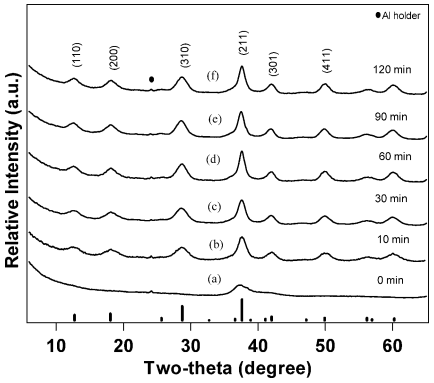

Figure 2. XRD patterns of K-OMS-2 prepared at different reflux times with 10% DMSO by total volume. The vertical solid lines below the pattern correspond to the positions of the Bragg reflections for the Q-phase of cryptomelane (KMn_8O_{16}: JCPDS No. 29-1020).

selective detector coupled to a HP 5890 Series II gas chromatograph equipped with a TCD detector through HP-1 (nonpolar cross-linked methyl siloxane) column with dimensions of 12.5 m × 0.2 mm × 0.33 μm.

Results

Formation and Crystallization of OMS-2 Nanomaterials. Cryptomelane-type OMS materials were prepared by the comproportionation between Mn^{2+} and MnO_4^- in mixed aqueous and nonaqueous solvents in acidic media. When $KMnO_4$ solution was added dropwise to the acidified $MnSO_4$ solution, the mixture turned light brown and eventually darkened producing a brown precipitate. The addition of a small amount of the cosolvent did not result in significant color change. The initial precipitate was collected and analyzed by XRD and was found to be poorly ordered, Figure 2a. Aging of the precursor mixture at room temperature or addition of the cosolvent did not cause phase transformation to OMS-2. The phase transformation with time of the initially poorly ordered manganese oxides to well-ordered crystalline OMS-2 were followed by X-ray diffraction. Figure 2b−f shows the X-ray diffraction patterns of K-OMS-2 prepared at different microwave reflux times with water and 10% (v/v) dimethyl sulfoxide (DMSO). The crystalline cryptomelane phase (JCPDS No. 29-1020) was formed within 10 min and the relative intensities of the diffraction peaks remained virtually unchanged with increased reflux time. The average crystallite size varied from 5.0 to 6.8 nm from 10 to 120 min. Experiments performed under similar conditions but utilizing a conventional oil-bath reflux method for 90 min did not yield phase pure cryptomelane-type OMS-2 materials. Mixed OMS-2 and hausmannite (Mn_3O_4, JCPDS 24-734) phases were obtained (Figure S2 in the Supporting Information).

Narrower OMS-2 nanomaterials were obtained by varying the amount of DMSO in the reaction mixture. Figure 3 shows the XRD patterns of K-OMS-2 prepared at different percent (v/v) DMSO for 90 min. Clearly, the peak broadness increased with increasing cosolvent concentrations. The average particle size of the resulting OMS-2 decreased systematically with increasing DMSO concentrations, Figure 4.

The X-ray diffraction patterns of materials obtained when other cosolvents are used are shown in (Figure S3, Supporting Information). When 10% sulfolane (tetramethylene sulfone) was utilized, highly crystalline pure OMS-2 materials were obtained in less than 10 min of microwave refluxing. The intensities of the sharper OMS-2 peaks did not change significantly with increasing reflux times (Figure S3(a) in the Supporting Information). The average particle diameter range was 17−19 nm.

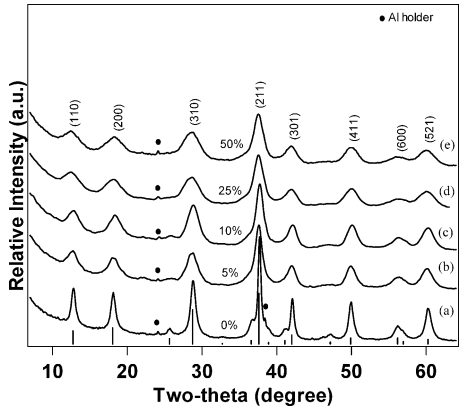

Figure 3. XRD patterns of K-OMS-2 prepared with different percent DMSO for 90 min.

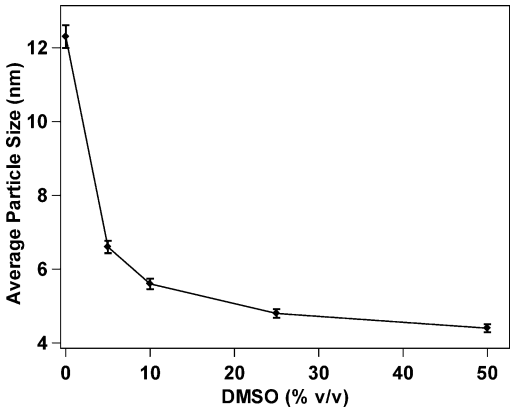

Figure 4. Average particle size of K-OMS-2 nanomaterials prepared by microwave reflux for 90 min as a function of DMSO concentration.

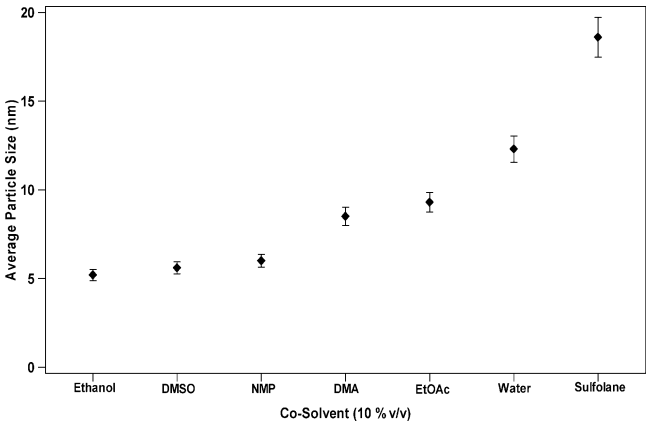

Figure 5. The effect of solvent on particle size of K-OMS-2 nanomaterials prepared by microwave reflux for 90 min. DMSO = dimethyl sulfoxide; NMP = *N*-methyl-2-pyrrolidone; DMA = dimethylacetamide; EtOAc = ethyl acetate; and sulfolane = tetramethylene sulfone.

However, when 10% ethyl acetate was used pure phase OMS-2 was not obtained in 10 min of microwave refluxing. A mixture of OMS-2 and γ-MnO_2 was observed (Figure S3b in the Supporting Information). Further microwave reflux aging up to 90 min yielded single-phase OMS-2 materials. The average particle size of cryptomelane produced under different cosolvents (ethanol, NMP, DMA, and sulfolane) varied from 5 to 20 nm, Figure 5. Use of 10% ethylene glycol and propylene glycol did not result in the formation of OMS-2 but instead the predominantly crystalline manganite phase (γ- MnOOH, JCPDS No. 41-1379) was obtained after 90 min of microwave refluxing in 10% glycol precursor mixture (Figure S4, Supporting

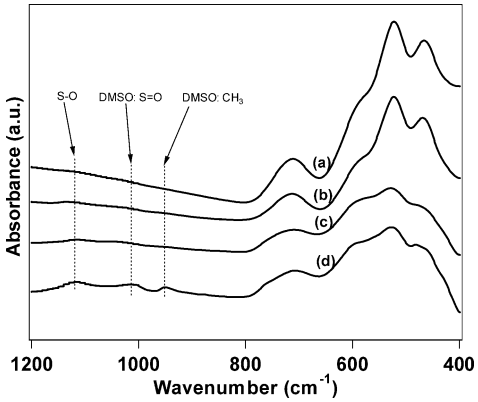

Figure 6. FT-IR spectra of cryptomelane materials prepared by (a) conventional reflux without DMSO for 24 h, (b) microwave-reflux with 0% DMSO, (c) microwave-reflux with 10% DMSO, and (d) microwave-reflux with 50% DMSO for 90 min.

Information). This phase is reported to form after extended periods (>4 h) in conventional reflux and hydrothermal processing under aqueous media.[11]

Representative Raman spectra of OMS-2 synthesized without cosolvent and with 10% DMSO are shown in (Figure S5 in the Supporting Information). The samples show a weak shoulder band around 580 cm^{-1} and a strong wide peak at approximately 640 cm^{-1}. These peaks are assigned to $F_{2g}{}^1$ and A_{1g} species, respectively. The strong A_{1g} vibration mode corresponds to the different vibration modes of $[MnO_6]$ octahedron. The shoulder peak ($F_{2g}{}^1$ mode) is due to the symmetric Mn−O stretching vibration of $[MnO_6]$ octahedron because of the structural differences between isotropic $[Mn^{4+}O_6]$ and the locally distorted $[Mn^{3+}O_6]$ octahedrons as suggested by Julien et al.[12]

Surface properties of cryptomelane nanomaterials prepared via microwave with mixed aqueous and nonaqueous solvents were studied by FT-IR, Figure 6. All the samples exhibit vibration modes typical to OMS-2 in the framework region between 800 and 400 cm^{-1}. However, the samples prepared with 50% (v/v) DMSO showed additional bands between 1200 and 800 cm^{-1}. The bands at ∼1120 and 1020 cm^{-1} could be attributed to S−O and S═O stretching of DMSO respectively. The peak around 950 cm^{-1} is assigned to the CH_3 rocking frequency of DMSO methyl groups.[13]

Morphology. Figure 7a shows the morphology of a poorly ordered manganese oxide precursor formed at room temperature after reaction between Mn^{2+} and MnO_4^- in aqueous and nonaqueous (10% DMSO) acidic media. Low-ordered manganese oxide chunks with particle diameters of about 100 nm were formed. Figure 7b−d displays FESEM images of K-OMS-2 with fibrous morphologies produced at different conditions. The FESEM images of cryptomelane material obtained after microwave-refluxing for 90 min without the use of any cosolvent are illustrated in Figure 7b. Well-formed needle-like morphologies are observed with an average diameter of 13 nm and a few hundred nanometers in length. Similar fibrous morphologies have been observed for bulk and nanosize OMS-2 materials prepared by reflux methods after prolonged processing times (>17 h). The OMS-2 nanomaterials produced with use of 10% DMSO had smaller and much shorter fiber bunches as observed in Figure 7c. Increasing the concentration of the cosolvent (50% DMSO) resulted in K-OMS-2 aggregated fiber bunches with narrower widths and shorter lengths, Figure 7d.

Figure 8 shows low- and high-resolution TEM images of OMS-2 synthesized in 10% DMSO mixture for 90 min under microwave refluxing. The TEM studies of these nanofibers,

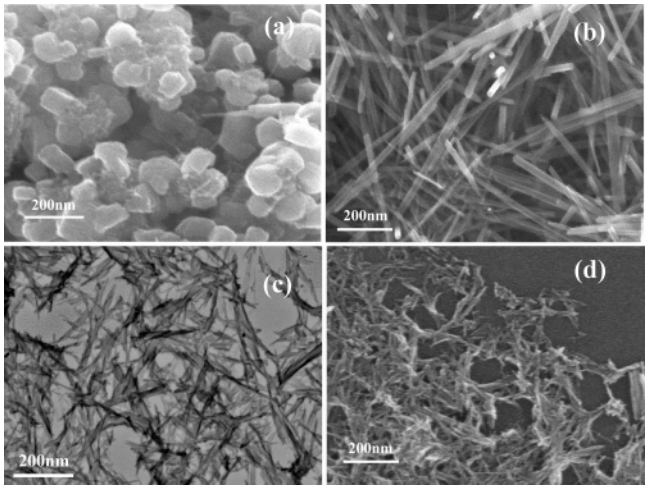

Figure 7. FESEM of (a) precursor without heating ($T = 0$ min) with 10% DMSO, (b) microwave-reflux without DMSO, (c) microwave-reflux with 10% DMSO, and (d) microwave-reflux with 50% DMSO for 90 min.

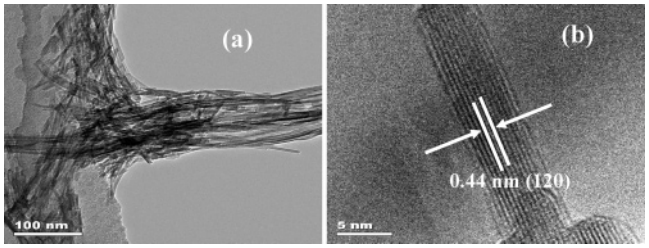

Figure 8. Low-resolution TEM and high-resolution TEM images of K-OMS-2 prepared by microwave reflux at 100 °C for 90 min in 10% DMSO.

Figure 8a, show uniform fibrous nanomaterials with an average diameter of 5.4 ± 0.3 nm (based on a count of ∼50 nanofibers), which is consistent with particle size analyses by XRD. These nanofibers exhibited well-defined lattice fringes of 0.44 nm and can be indexed to the (120) planes as recently reported by Portehault and co-workers.[6a] The lattice planes confirmed the excellent crystallinity of the sample.

Thermal Stability. Thermal stabilities of K-OMS-2 nanomaterials synthesized by microwave-reflux were studied by using TGA and DSC. The TGA plots of materials prepared for 90 min at different cosolvent (DMSO) concentrations (0−50%) are shown in Figure 9. There are three major weight losses in the TGA profiles of samples prepared with low cosolvent concentrations (<25% v/v). However, OMS-2 nanomaterials prepared at high DMSO concentration (50% v/v) show four weight losses between 30 and 900 °C in inert atmosphere. The first weight loss (∼4%) for the sample prepared with no cosolvent (100% water) occurs between 30 and 250 °C. This is attributed to physically adsorbed water molecules on the surface of the material. The second TGA weight loss (∼6%) for this sample between 400 and 620 °C is ascribed to the evolution of oxygen and chemically bound water molecules from the OMS-2 material, as reported previously.[2,5h] The third weight loss of ∼3% is due to the second lattice oxygen release at 620−750 °C. All samples except those prepared with 50% v/v DMSO concentration showed a similar TGA plot with only slight differences in the weight loss range. Similar thermal behavior has been previously observed for OMS-2 materials.[2,5h] The cryptomelane sample prepared with 50% DMSO shows a different TGA profile, particularly between 100 and 440 °C accounting for a 6% weight loss. The weight losses around 100 and 190 °C were accompanied by endothermic peaks in DSC

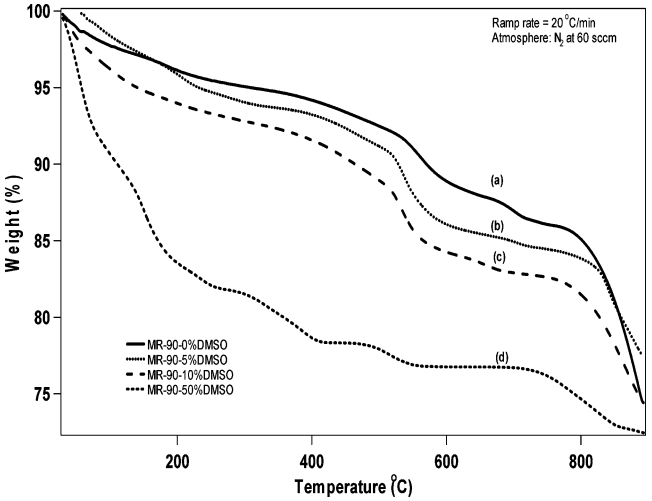

Figure 9. TGA profiles for K-OMS-2 nanomaterials prepared at different DMSO concentrations (0−50% v/v).

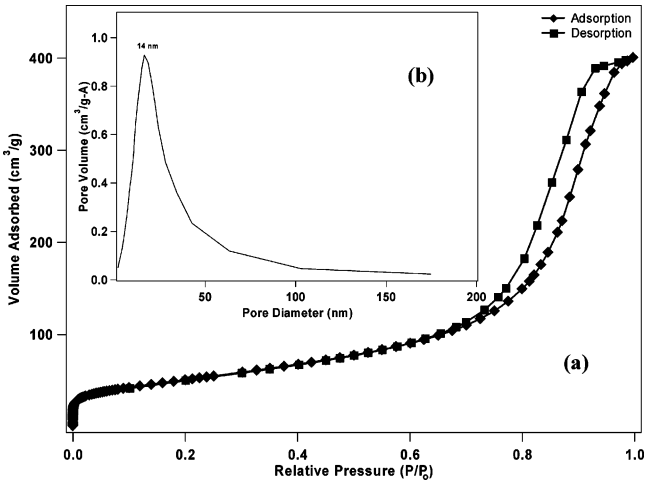

Figure 10. (a) N_2 adsorption/desorption isotherms and (b) Barrett−Joyner−Halenda (BJH) prepared by microwave reflux at 100 °C for 90 min in 10% DMSO.

at 100 and 190 °C, which correspond to the boiling point of water and DMSO, respectively (Figure S6, Supporting Information). The peaks are attributed to physical desorption of water and DMSO from the surface. The exothermic peak at 370 °C associated with a 4% weight loss at ca. 400 °C could be assigned to desorption/decomposition of moieties on the surface of OMS nanofibers. The weight loss at >750 °C has been assigned to the evolution of structural oxygen in the framework of the tunnels.[2]

Surface Area and Porosity. Figure 10 shows a representative N_2 adsorption/desorption isotherms of OMS-2 nanomaterials obtained via microwave reflux in mixed aqueous and nonaqueous media. All the samples exhibited a type II adsorption isotherm according to IUPAC classification.[10] At low relative pressure (P/P_o) formation of a monolayer of adsorbed molecules is the prevailing process, while at high P/P_o a multilayer of adsorption takes place. This type of isotherm is similar to those observed for OMS-2 materials prepared by other synthetic methods.[2,5]

The Brunauer−Emmett−Teller (BET) surface area of the synthesized OMS-2 nanomaterials ranged from 89 to 227 m^2/g and in general increased with increasing cosolvent concentration and microwave-reflux time, Table 1. The surface area and total pore volume of the representative sample (MR-90−10% DMSO) were 214 ± 1 m^2/g and 0.62 cm^3/g and are much higher than

TABLE 1: BET Surface Area of K-OMS-2 Materials

sample	$S_{BET} \pm 1$ (m^2/g)	sample	$S_{BET} \pm 1$ (m^2/g)
MR-90−10%DMSO	214	MR-90−50%DMSO	188
MR-60−10%DMSO	187	MR-120−10%DMSO	158
MR-30−10%DMSO	143	MR-120−0%DMSO	99
MR-10−10%DMSO	223	precursor-10%DMSO	89
MR-90−0%DMSO	98	conv. reflux[a]	91
MR-90−5%DMSO	173	1% H_2O_2 reflux[b]	62
MR-90−25%DMSO	227		

[a] Reference 5h. [b] Reference 2.

TABLE 2: Conversion and Selectivity of Anisyl Alcohol to Anisyl Aldehyde with Use of OMS-2 Prepared with Different Cosolvent Concentrations

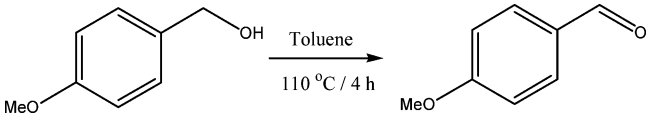

catalyst	conversion,[a] ±2%	selectivity,[a] %
MR-120−10% DMSO	77.3	100
MR-90−10% DMSO	79.1	100
MR-120−0% DMSO	74.9	100
MR-90−50% DMSO	3.56	100
MR-10−10% DMSO	94.9	100
conventional OMS[b]	62.8	100

[a] Product identification and quantification by GC-MS. MR = microwave reflux. [b] Conversion of OMS-2 prepared via traditional oil-bath refluxing for 24 h without DMSO.[5c]

those of K-OMS-2 prepared by conventional oil-bath reflux of 90 m^2/g and 0.46 cm^3/g, respectively.[5h] The BJH average pore diameter of 14 nm confirms the mesoporous nature of the material, Figure 10b inset) and is lower than that of conventionally prepared K-OMS-2 of 20.3 nm.[5h] These mesopores contribute to a large extent to the total pore volume of the samples and may play a role in the catalytic activity of OMS-2.[14] Previous work showed that these mesopores consist of slit-shaped pores with nonuniform shapes and sizes.[2] The material also shows a sharp peak of ~0.52 nm that reveals the microporous structure of this sample (Figure S7, Supporting Information). However, the contribution of these micropores to the total pore volume was not significant.

Catalytic Activity of OMS-2 Nanofibers. OMS-2 materials have been found to exhibit excellent catalytic activities in several applications with interest to fine chemical industry and academia.[2,5] The catalytic performance of OMS-2 nanofibers prepared via microwave-reflux with and without cosolvents was investigated in the oxidation of anisyl alcohol to anisyl aldehyde. For comparison, OMS-2 materials prepared with the conventional oil-bath reflux method were also evaluated. The synthesized K-OMS-2 nanomaterials showed excellent catalytic activities in oxidation of anisyl alcohol to anisyl aldehyde. All the evaluated catalysts showed 100% selectivity to anisyl aldehyde. The conversion and selectivity results are summarized in Table 2. For the oxidation of anisyl alcohol, a 63% conversion was obtained when regular OMS-2 catalyst prepared by conventional reflux method was used. With the exception of catalysts prepared with 50% DMSO for 90 min, microwave reflux prepared K-OMS-2 catalysts showed higher catalytic activities than that of catalysts prepared by conventional oil-bath refluxing methods. OMS-2 prepared in 10 min via the microwave-reflux method with 10% DMSO showed a remarkable conversion of 95%. However, OMS-2 prepared at high

TABLE 3: Dielectric Constant, Dielectric Loss, and tan δ of Different Solvents[7]

solvent	dielectric constant[a]	dielectric loss[a]	tan δ
ethylene glycol	37.00	49.95	1.35
ethanol	24.30	22.87	0.94
DMSO	45.00	37.12	0.83
NMP	32.20	8.86	0.28
DMA	37.80	nd	nd
DMF	37.70	6.07	0.16
Water	80.40	9.89	0.12
ethyl acetate	6.00	0.35	0.06
sulfolane	44.00	nd	nd

[a] Measured at 20 °C and 2.45 GHz. nd: no data available.

DMSO concentrations, i.e., 50% (v/v), displayed extremely low catalytic activity, 4%.

Discussion

Formation of K-OMS-2 Nanofibers. In this work, microwave synthesis of OMS-2 materials in mixed aqueous and nonaqueous solvents was conducted in an open-vessel by the reflux method. In acidic media, the reduction potentials of MnO_4^-/Mn^{4+} and Mn^{2+}/MnO_2 are 1.69 and 1.23 V, respectively.[6,15] Hence, a spontaneous redox reaction occurs between the reactants dissolved in water. Portehault et al. recently showed by volumetric titration that about 99% of $KMnO_4$ had reacted with 91% of $MnSO_4$ within 10 min of the reactants mixing.[6] As the reaction proceeds, Mn^{2+} is oxidized by potassium permanganate and the color turns immediately from light pink to light brown and finally a dark brownish precipitate is obtained. This color remained essentially unchanged with the addition of a small amount of a nonaqueous cosolvent. Different cosolvents grouped according to their ability and efficiency to convert microwave energy into heat were investigated. A reaction medium with a high loss factor (tan δ) value is needed for efficient absorption and, consequently, for rapid heating. Table 3 shows the dielectric constant (ϵ'), dielectric loss (ϵ''), and loss factor (tan δ) for solvents used in this research. In general, the loss factor (tan δ) decreases with temperature but the trend essentially remains unchanged for the solvents used in this study at 100 °C.[7c] Solvents such as ethylene glycol, ethanol, and DMSO are considered high microwave absorbers, while NMP, DMF, DMA, and water are medium absorbers. Ethyl acetate with the lowest tan δ value does not couple very efficiently to microwave irradiation and will not super heat rapidly.

The influences of the cosolvent type and reflux time on the crystallization of OMS-2 nanomaterial were investigated by comparing the XRD patterns of the materials prepared at different conditions, Figure 2. XRD patterns indicate that the initial MnO_x precipitate obtained after the reaction between potassium permanganate and manganese sulfate monohydrate in mixed aqueous and 10% (DMSO) nonaqueous solvents are poorly ordered. Upon microwave refluxing for 10 min the poorly ordered manganese oxide transformed rapidly to a well-crystallized phase pure tunnel-type OMS-2 nanomaterial. The peak widths were significantly broad, an indication of small particle sizes. The relative intensities of the diffraction peaks and particle size of the samples did not change significantly with increased microwave-reflux time from 10 to 120 min. This indicates that pure stable cryptomelane nanomaterial with an ordered tunnel structure (0.46 nm × 0.46 nm) is formed rapidly in less than 10 min. Other methods require longer processing times ranging from 4 to 24 h.[2] The rapid nucleation of K-OMS-2 nanomaterials prepared by the microwave reflux route utilizing selective heating of polar solvents such as DMSO in the reactant mixture is attributed to the local superheating of the reactant mixture. The presence of DMSO restricts lateral aggregation of OMS-2 nanofibers and hence narrower fiber diameters are obtained. Reactions performed with low microwave absorbing solvents (water and ethyl acetate) required longer reaction times to form pure phase crystalline OMS-2 as evidenced by the XRD patterns for 10% ethyl acetate in Figure S3a (Supporting Information). After 10 min of microwave refluxing a mixture of OMS-2 and γ-MnO_2 are obtained. Solvents such as sulfolane resulted in faster crystallization of OMS-2 with sharper XRD peak intensities, Figure S3b (Supporting Information). In sulfolane the formation process is dominated by lateral crystal growth. Use of glycols (ethylene and propylene glycol) as cosolvents in the concentration between 5% and 10% resulted in the formation of the manganite (γ-MnOOH) phase, as observed in Figure S4 (Supporting Information). This suggests that although glycols have a high loss factor, their reducing power could reduce Mn^{4+} to Mn^{3+} leading to the formation of the manganite phase. The other systems have less reducing power and comproportionation of Mn^{3+} to Mn^{4+}/Mn^{2+} species is accomplished leading to the formation of OMS-2 and suppression of the manganite phase. This shows that the type of cosolvent affects nucleation of OMS-2 materials and OMS-2 will only be obtained with optimized interactions between the solvent and the reacting species.

Systematic Particle Size Control of OMS-2 Nanomaterials. Systematic particle control of OMS-2 nanomaterials is not trivial. In this work, the average OMS-2 fiber diameters were affected by the concentration of the nonaqueous solvent in the initial reaction mixture as evidenced by the XRD peak broadening, and the electron microscopy in Figure 3 and Figures 7 and 8, respectively. OMS-2 fiber diameters were found to decrease systematically with increasing DMSO concentration from 0 to 50% (v/v), Figure 4. The presence of the high loss factor (tan δ) solvent DMSO in the mixture under microwave irradiation leads to the formation of hot spots that serve as nucleation sites. Nucleation of cryptomelane crystals occurs rapidly producing nanomaterials with very narrow fiber diameters. Under microwave heating, once the amount of DMSO is increased, the available reactants are consumed quickly resulting in even smaller nanocrystals. The decrease of fiber diameter with increased DMSO percent could also be explained by the limited lateral aggregation of the OMS-2 nanofibers due to the presence of functional groups from the cosolvent such as S═O from DMSO, which could form weak H-bonding with the surface −OH groups from the manganese oxide nanofibers. This is consistent with FT-IR, TGA, and DSC results, Figure 6, Figure 9, and Figure S6 (Supporting Information), respectively.

Control of the diameter of OMS-2 nanofibers was also accomplished by using different cosolvent in the reaction mixture. A variety of solvents which include dimethylformamide (DMF), dimethylacetamide (DMA), *N*-methylpyrrolidone (NMP), ethanol, dimethyl sulfoxide (DMSO), and tetramethylene sulfone (sulfolane) were employed in this work. The OMS-2 fiber diameter increased in the order of ethanol > DMSO > NMP > DMA > EtOAc > H_2O > sulfolane. This trend correlated well with the loss factor (tan δ) of the nonaqueous solvents. This means that the higher the loss factor the lower the average particle size of the obtained K-OMS-2 as illustrated in Figure 5.

Morphology and Textural Properties. The OMS-2 materials synthesized by the microwave-reflux method with mixed

aqueous and nonaqueous solvents show uniform fibrous morphology, Figures 7 and 8. This type of morphology is typical of cryptomelane materials prepared via reflux methods.[2] Fibers with narrow diameters as low as 5 nm were synthesized by the method reported here and have smaller diameters than those prepared by conventional reflux methods.[2,5h,6] The fiber diameters calculated from XRD line broadening correlated well with those calculated from TEM images. HRTEM reveal well-defined lattice planes that confirm the excellent crystallinity of the samples.

Textural properties of the samples prepared via microwave-reflux are similar to those observed for K-OMS-2 prepared by other methods.[2] The Brunauer−Emmett−Teller (BET) surface area and total pore volume of microwave-reflux sample were 214 ± 1 m^2/g and 0.62 cm^3/g and are much higher than those of K-OMS-2 prepared by conventional oil-bath reflux of 90 m^2/g and 0.46 cm^3/g, respectively.[5h] The BJH average pore diameter of 14 nm confirms the mesoporous nature of the material and is lower than that of conventionally prepared K-OMS-2 of 20.3 nm. A reviewer suggested that dispersion of the catalyst in reaction mixture may eliminate the effects of mesoporosity in the catalytic activity of OMS-2. The material also shows a sharp peak of 0.52 nm, which is close to the tunnel size of 4.6 Å for OMS-2 and reveals the microporous structure of the sample. However, the contribution of these micropores to the total pore volume was not significant. In general, the surface area increased with increasing aging time and cosolvent concentration. This is attributed to the formation of longer nanofibers with increased reflux time and limited lateral growth rate with increased cosolvent concentration, producing ultranarrow fibers with high aspect ratios. Further surface and structural investigations with ^{13}C, ^{1}H NMR and synchrotron XRD are underway.

Catalytic Applications. The synthesized K-OMS-2 nanomaterial showed excellent catalytic activities in the oxidation of anisyl alcohol to anisyl aldehyde, Table 2. All the tested catalysts show 100% selectivity to anisyl aldehyde. With the exception of catalysts prepared at 50% DMSO for 90 min, microwave reflux prepared K-OMS-2 catalysts have higher catalytic activities than that of catalysts prepared by conventional oil-bath refluxing methods. At high DMSO concentrations, i.e., 50% (v/v), the solvent molecules were probably confined in the pores between the particles or bound to the particle surface blocking some catalytically active sites, which led to low catalytic activities. Optimization of interactions between the stabilizing agents and the metal surfaces is critical to preserving catalytically active sites. When interactions between the stabilizing agent and the metal surface are too strong, the catalytic activity is expected to decrease tremendously.[16] This is consistent with FT-IR, TGA, and DSC results, Figure 6, Figure 9, and Figure S6 (Supporting Information), respectively. Further catalyst characterization and elucidation of the role of OMS-2 in the oxidation of anisyl alcohol are ongoing.

Conclusion

Size tunable (4−20 nm), high surface area (>200 m^2/g) cryptomelane-type OMS-2 nanomaterials were rapidly prepared via an open-vessel microwave-reflux route in mixed aqueous and nonaqueous solvents. The particle size control was accomplished by adjusting the amount of the cosolvent in the reactant mixture or by using different cosolvents. Materials produced via the reported method show remarkable catalytic activity in the oxidation of anisyl alcohol to the corresponding anisyl aldehyde when compared to catalysts prepared by conventional reflux conditions. The advantages of this route include rapid, reproducible, and efficient production of phase pure ultranarrow K-OMS-2 nanofibers with controllable particle sizes (4−20 nm), very high surface areas up to 227 m^2/g, and excellent catalytic activity when compared with that of conventional OMS-2 catalyst. In addition, this route is of commercial interest as multigram quantities of OMS-2 nanomaterials are produced rapidly under ambient pressures and could result in significant energy savings.

Acknowledgment. We acknowledge support of NSF under NIRT award CTS-0304217. We thank Naftali Opembe and Linping Xu for their help. Special thanks go to Dr. Francis S. Galasso for helpful discussions and comments.

Supporting Information Available: Photograph of the microwave-reflux setup and additional characterization. This material is available free of charge via the Internet at http://pubs.acs.org.

References and Notes

(1) (a) Law, M.; Goldberger, J.; Yang, P. *Annu. Rev. Mater. Sci.* **2004**, *34*, 83. (b) Mokari, T.; Zhang, M.; Yang, P. *J. Am. Chem. Soc.* **2007**, *129*, 9864. (c) Goldberger, J.; Fan, R.; Yang, P. *Acc. Chem. Res.* **2006**, *39*, 239. (d) Efros, A. L.; Rosen, M. *Annu. Rev. Mater. Sci.* **2000**, *30*, 473−521. (e) Lieber, C. M. *MRS Bull.* **2003**, *28*, 486. (f) Lombardi, I.; Hochbaum, A. I.; Yang, P.; Carrano, C.; Maboudian, R. *Chem. Mater.* **2006**, *18*, 988. (g) Sirbuly, D.; Law, M.; Yan, H.; Yang, P. *J. Phys. Chem. B* **2005**, *109*, 15190. (h) Yang, L.-X.; Zhu, Y.-J.; Wang, W.-W.; Tong, H.; Ruan, M.-L. *J. Phys. Chem. B* **2006**, *110*, 6609. (i) Shen, X. F.; Ding, Y. S.; Liu, J.; Cai, J.; Laubernds, K.; Zerger, R. P.; Vasiliev, A.; Aindow, M.; Suib, S. L. *Adv. Mater.* **2005**, *17*, 805.

(2) Villegas, J. C.; Garces, L. J.; Gomez, S.; Durand, J. P.; Suib, S. L. *Chem. Mater.* **2005**, *17*, 1910.

(3) (a) Panda, A. B.; Glaspell, G.; El-shall, S. *J. Am. Chem. Soc.* **2006**, *128*, 2790. (b) Huynh, W. U.; Dittmer, J. J.; Alivisatos, A. P. *Science* **2002**, *295*, 2425. (c) Duan, X.; Huang, Y.; Cui, Y.; Wang, J.; Lieber, C. M. *Nature* **2001**, *409*, 66. (d) Frank, S.; Poncharal, P.; Wang, Z. L.; de Heer, W. A. *Science* **1998**, *280*, 1744. (e) Huang, H. M.; Mao, S.; Feick, H.; Yan, H.; Wu, Y.; Kind, H.; Weber, E.; Russo, R.; Yang, P. *Science* **2001**, *292*, 1897. (f) Yuhas, B. D.; Zitoun, D. O.; Pauzauskie, P. J.; He, R.; Yang, P. *Angew. Chem., Int. Ed.* **2006**, *45*, 420. (g) Martin, C. R. *Science* **1994**, *266*, 1961. (h) Ma, R.; Bando, Y.; Sasaki, T. *J. Phys. Chem. B* **2004**, *108*, 2115. (i) Sun, Y.; Xia, Y. *Adv. Mater.* **2004**, *16*, 264.

(4) (a) Post, J. E. *Proc. Natl. Acad. Sci. U.S.A.* **1999**, *96*, 3447−3454. (b) Post, J. E.; Burnham, C. W. *Am. Mineral.* **1986**, *71*, 1178. (c) Feng, Q.; Kanoh, H.; Miyai, Y.; Ooi, K. *Chem. Mater.* **1995**, *7*, 148.

(5) (a) Son, Y. C.; Makwana, V. D.; Howell, A. R.; Suib, S. L. *Angew. Chem., Int. Ed.* **2001**, *40*, 4280. (b) Shen, Y. F.; Zerger, R. P.; DeGuzman, R. N.; Suib, S. L.; McCurdy, L.; Potter, D. I.; O'Young, C. L. *Science* **1993**, *260*, 511. (c) DeGuzman, R. N.; Shen, Y. F.; Neth, E. J.; Suib, S. L.; O'Young, C. L.; Levine, S.; Newman, J. M. *Chem. Mater.* **1994**, *6*, 815. (d) Chen, X.; Shen, Y. F.; Suib, S. L.; O'Young, C. L. *J. Catal.* **2001**, *197*, 292. (e) Xia, G.-G.; Tong, W.; Tolentino, E. N.; Duan, N.-G.; Brock, S. L.; Wang, J.-Y.; Suib, S. L.; Ressler, T. *Chem. Mater.* **2001**, *13*, 1585. (f) Shen, X. F.; Ding, Y. S.; Liu, J.; Laubernds, K.; Zerger, R. P.; Polverejan, M.; Son, Y. C.; Aindow, M.; Suib, S. L. *Chem. Mater.* **2004**, *16*, 5327. (g) Suib, S. L. *Annu. Rev. Mater. Sci.* **1996**, *26*, 135. (h) Ding, Y.-S.; Shen, X.-F.; Sithambaram, S.; Gomez, S.; Kumar, R.; Crisostomo, V. M. B.; Suib, S. L.; Aindow, M. *Chem. Mater.* **2005**, *17*, 5382. (i) Zhang, Q.; Luo, J.; Vileno, E.; Suib, S. L. *Chem. Mater.* **1997**, *9*, 2090. (j) Kim, S. H.; Kim, S. J.; Oh, S. M. *Chem. Mater.* **1999**, *11*, 557. (k) Ching, S.; Roark, J. L. *Chem. Mater.* **1997**, *9*, 750. (l) Jothiramalingam, R.; Viswanathan, B.; Varadarajan, T. K. *Catal. Commun.* **2005**, *6*, 41. (m) Feng, Q.; Kanoh, H.; Miyai, Y.; Ooi, K. *Chem. Mater.* **1995**, *7*, 148. (n) Sauvage, F.; Baudrin, E.; Tarascon, J.-M. *Sens. Actuators, B* **2007**, *120*, 638. (o) Kijima, N.; Takahashi, Y.; Akimoto, J.; Awaka, J. J. *Solid State Chem.* **2005**, *178*, 2741.

(6) (a) Portehault, D.; Cassaignon, S.; Baudrin, E.; Jolivet, J.-P. *Chem. Mater.* **2007**, *19*, 5410. (b) Garces, L. J.; Hincapie, B.; Makwana, V. D.; Laubernds, K.; Sacco, A.; Suib, S. L. *Microporous Mesosporous Mater.* **2003**, *63*, 11. (c) Liu, J.; Son, Y. C.; Cai, J.; Shen, X.; Suib, S. L.; Aindow, M. *Chem. Mater.* **2004**, *16*, 276.

(7) (a) Tompsett, G. A.; Conner, W. C.; Yngvesson, K. S. *ChemPhysChem* **2006**, *7*, 296. (b) Kappe, C. O. *Angew. Chem., Int. Ed.* **2004**, *43*, 6250. (c) Hayes, B. L. *Microwave Synthesis*: *Chemistry at the Speed of Light*; CEM Publishing: Mathews, NC, 2002. (d) Tierney, J. P.; Lidström, P. *Microwave Assisted Organic Synthesis*; CRC Press: Boca Raton, FL,

2005. (e) Nyutu, E. K.; Conner, W. C.; Auerbach, S.; Chun-Hu, C.; Suib, S. L. *J. Phys. Chem. C* **2008**, *112*, 1407.

(8) IUPAC Compendium of Chemical Terminology, Electronic version, http://goldbook.iupac.org/C01217.html.

(9) (a) Klug, H.; Alexander, L. *X-ray Diffraction procedures*; Wiley: New York, 1962; p 125. (b) Cullity, B. D.; Stock, S. R. *Elements of X-Ray Diffraction*; Prentice Hall: Upper Saddle River, NJ, 2001; p 170.

(10) (a) Sing, K. S. W.; Everett, D. H.; Haul, R. A. W.; Moscou, L.; Pierotti, R. A.; Rouquerol, J.; Siemieniewska, T. *Pure Appl. Chem.* **1985**, *57*, 603. (b) Leofanti, G.; Padovan, M.; Tozzola, G.; Venturelli, B. *Catal. Today* **1998**, *41*, 207.

(11) Crisostomo, V. M. B.; Ngala, J. K.; Alia, S.; Dobley, A.; Morein, C.; Chen, C.-H.; Shen, X.; Suib, S. L. *Chem. Mater.* **2007**, *19*, 1832.

(12) Julien, C. M.; Massort, M. *Mater. Sci. Eng., B* **2003**, *97*, 217.

(13) Elbaum, R.; Vega, S.; Hodes, G. *Chem. Mater.* **2001**, *13*, 2272.

(14) Ghosh, R.; Xiong-fei, S.; Villegas, J. C.; Ding, Y.; Malinger, K.; Suib, S. L. *J. Phys. Chem. B* **2006**, *110*, 7592.

(15) Antelman, M. S. *The Encyclopedia of Chemical Electrode Potentials*; Plenum Press: New York, 1982.

(16) Lee, H.; Habas, S. E.; Kweskin, S.; Butcher, D.; Somorjai, G. A.; Yang, P. *Angew. Chem., Int. Ed.* **2006**, *45*, 7824.